Published in Surface Science 395, issue 1, 120-129, 1998
which should be used for any reference to this work

Structural characterization of submonolayer C/Al(111)

S. Scalese *, R.G. Agostino, J. Hayoz, D. Naumovič, R. Fasel, P. Aebi, L. Schlapbach

Institut de Physique, Université de Fribourg, CH-1700 Fribourg, Switzerland

Abstract

We report on the adsorption of atomic C in submonolayer coverages on the Al(111) surface. The local order at the surface is studied for different thermal treatments by means of full-heimispherical X-ray photoelectron diffraction. Deposition at room temperature results in disordered C adsorption while an ordering process takes place after annealing above 475 K. We depict the structure of the annealed C-rich phase. The C1s diffraction patterns are interpreted by comparison with single scattering cluster calculations. The results are discussed with respect to both previous theoretical and experimental work.

Keywords: Aluminum; Carbon; Diamond; Diffusion and migration; Low index single crystal surfaces; Photoelectron diffraction; Surface structure

1. Introduction

In the past, adsorption of light atoms on metal surfaces has received wide attention because of being involved in several processes such as catalysis, corrosion, oxidation and thin film growth. Despite the attention paid to alkali atom-, water- and oxygen-adsorption on Al surfaces [1–5], the literature on C adsorption is very scarce. A theoretical study [6] describes, in an equivalent way, C and O adsorption on Al(100) with both atoms strongly bound to a four-fold site above the Al surface plane. In another theoretical study [7] it is found that for O/Al(111) the O atoms are adsorbed in the three-fold site 0.60 ± 0.10 Å above the surface and no indication is given for preferred hcp or fcc site occupation. A scanning tunneling microscopy (STM) study [8] performed on residual C atoms on an Al(111) surface, shows that C is located in the hcp three-fold site. From this experimental study it is not possible to establish whether or not the C atoms diffuse into the substrate and if the apparent displacement of the Al atoms around an adsorbed C atom is real or due to a local variation of the electronic density of states induced by the bonding configuration.

Recently, a density functional theory study [9] reports on two nearly degenerate subsurface adsorption sites: a six-fold coordination site halfway between the first and second Al layer and a slightly distorted tetrahedral site 0.2 Å below the unrelaxed Al surface. The tetrahedral sites can be preferentially populated because they have no access potential barrier. In thermodynamic equilibrium the two sites can be nearly equally populated because of the small difference in energy.

Here we study the C/Al(111) system using full-hemispherical X-ray photoelectron diffraction

* Corresponding author. Present address: Dipartimento di Fisica, Università della Calabria, I-87036 Arcavacata di Rende, Italy. E-mail: scalese@fermi.fis.unical.it

(XPD) which is a well-established, surface-sensitive structural tool [10]. Following the angular intensity distribution of the C 1s photoemission line, we are able to investigate the local order around the C atoms. At the electron kinetic energy of the C 1s emission line ($E_{kin}=970$ eV) the photoelectron scattering process is dominated by the *forward focusing* effect, i.e. the photoelectron emitted from an atom is focused by its neighbors in forward directions [10]. The angular photoelectron intensity maps then show maxima in correspondence with the high symmetry directions where intensity is enhanced by close packed atomic rows [10–12].

In the present study the dependence on the diffusion of C on coverage and sample annealing temperature is investigated. The diffraction patterns are discussed using single scattering cluster (SSC) calculations [13,14]. Several structures of the C/Al(111) surface are tested. The comparison of the calculated patterns with the experiment shows that C atoms are embedded in a three-dimensional ordered C phase formed by annealing a C submonolayer deposited at room temperature (RT). The local structure of the C atoms is compatible with a zincblende environment in registry with the substrate. We suggest that surface diffusion and C–Al clustering are the main mechanisms for the formation of this structure. Results are compared with both, previous theoretical predictions and experiments.

2. Experimental

The deposition and analysis system is based on a modified Vacuum Generator ESCALAB Mk II spectrometer [15,16] with a base pressure of 2×10^{-11} mbar, equipped with a three channeltron hemispherical electron energy analyzer, a Mg Kα and Si Kα twin anode X-ray source, a quadrupole mass spectrometer and a low energy electron diffraction (LEED) system.The angle between X-ray source and analyzer is 54°.

During analysis the sample is mounted on an *xyz* manipulator with two rotational axes. Rotations are motoirized and computer controlled such that the photoelectron emission angles θ (polar angle, with respect to the normal) and ϕ (azimuthal angle) can be swept over the whole hemisphere above the sample and a series of spectra can be recorded automatically on a predetermined set of angles (θ,ϕ). The $\phi=0°$ azimuth corresponds to the $[11\bar{2}]$ direction of the Al(111) surface. The experimental procedure consists of the acquisition of the Mg Kα excited C 1s and Al 2p X-ray photoelectron intensity for each (θ,ϕ) setting. Data acquisition starts at $\theta=78°$ and stops at $\theta=0°$. The azimuthal step size at any polar angle is chosen so that the sampling density in solid angle is uniform. Up to 5000 measuring points are recorded with a total energy resolution of 1.4 eV. The intensity maps, $I(\theta,\phi)$, are stereographically projected using a linear gray scale representation. Normal emission appears in the center while grazing emission is plotted towards the border. The sample temperature was monitored using a thermocouple in contact with the surface.

The sample was cleaned by cycles of Ar^+ sputtering (1.5–0.5 keV) of the hot sample (575 K) and subsequent annealing to 700 K. Al(111) surface cleanness and order were checked by X-ray photoelectron spectroscopy and LEED, respectively. In particular, no C and O contamination was detected after this cleaning procedure.

C was deposited by direct resistive heating of a C thin strip (Goodfellow, 99.8%) while the source body was liquid-nitrogen cooled. The typical residual gas pressure during the evaporation was lower than 2×10^{-9} mbar. The C evaporation rate was measured by a quartz-balance placed beside the sample surface.

X-ray photoelectron spectra of the deposited C films showed very low contamination consisting mainly of O (<0.04 ML).

3. Results

Typical C 1s emission spectra from submonolayer C films that are deposited at RT and annealed at different temperatures are shown in Fig. 1. Spectra were acquired with a total energy resolution of 0.9 eV. The two components, clearly present at RT, are centered at 284.1 eV and

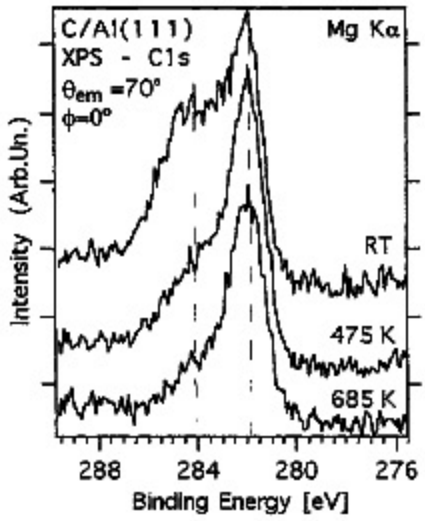

Fig. 1. X-ray photoelectron spectra of C 1s emission line (using Mg Kα radiation) obtained for submonolayer C films on Al(111) deposited at RT and after annealing at different temperatures. The polar angle between the analyzer entrance slits and the surface normal direction is $\theta_{em}=70°$. Two vertical dotted lines are traced as a guide to the eye and mark the position of the C 1s components.

281.9 eV binding energy, respectively. The higher binding energy component practically disappears under annealing and only a small shoulder remains at 685 K. We are not able to attribute each component to an exact C atom chemical environment. Nevertheless, the existence of a clear splitting of the C 1s peak indicates that after RT deposition two species are present at the surface, i.e. two different chemical bondings of C, while only one of them remains upon annealing at temperatures above 475 K. We are then in the presence of a thermally activated process that is correlated with major structural changes, as we will show in the following.

We performed our investigations on submonolayer films for which the normal emission intensity ratio I_{C1s}/I_{Al2p} is ranging between 0.03 and 0.19. If we consider a C density and a C–C nearest neighbor distance similar to the one for diamond, the corresponding coverage ranges from 0.05 to 0.21 ML.[1]

[1] The coverages are calculated assuming all the C atoms within the top surface layer. This is justified by the finding that no diffusion towards the bulk takes place upon deposition at RT.

A first structural investigation is performed by LEED (not shown) after deposition at RT and after annealing. Apart from the Al(111) surface diffraction spots, we do not find any extra feature in the patterns except that the background intensity is higher. Thus, a certain amount of long-range disorder characterizes the C/Al(111) surface. However, previous theoretical [9] and experimental [3] studies point to a locally ordered C atom adsorption, as we will discuss below.

From the C 1s XPD patterns of C deposited at RT (not shown) we find that no local order is present around the C atoms. In fact, all the patterns acquired at different coverages are dominated by a smooth polar-angle dependence of the intensities and there are no typical diffraction features indicating a C enviromnent which is equally ordered with respect to the Al substrate. We deduce that for RT deposition neither of the two kinds of C atoms which coexist on the surface in similar quantities (Fig. 1), exhibit local ordering with respect to the substrate.

In Fig. 2 we show the C 1s XPD patterns for C films deposited at RT and annealed at 375 K (a), 475 K (b) and 685 K (c). A smooth background is removed from the patterns in order to enhance the contrast of the diffraction features. Furthermore, we performed a three-fold averaging of the data according to the symmetry of the system. As a reference for the substrate directions, the Al 2p XPD pattern is shown in Fig. 2d. In all the C 1s XPD patterns we find intensity maxima along various directions going from grazing to normal emission. In particular, as marked in Fig. 2c, we find maxima at $\theta=72°$ (A) and $\theta=38°$ (B) in the $\phi=0°$ azimuth and at $\theta=81°$ (C), $\theta=54°$ (D) and a broad maximum between $\theta=21°$ and $\theta=40°$ (E) in the $\phi=60°$ azimuth. A maximum (F) is also present along the normal. Increasing the annealing temperature and carbon coverage, the contrast of these structures becomes higher but no new features appear.

Because of the forward focusing of the C 1s photoelectrons, the presence of maxima indicates local order around the C atoms [10]. Furthermore, the maxima near the surface normal point to C atom diffusion or to the formation of a bulk-like structure (i.e. the C emitters are burried below

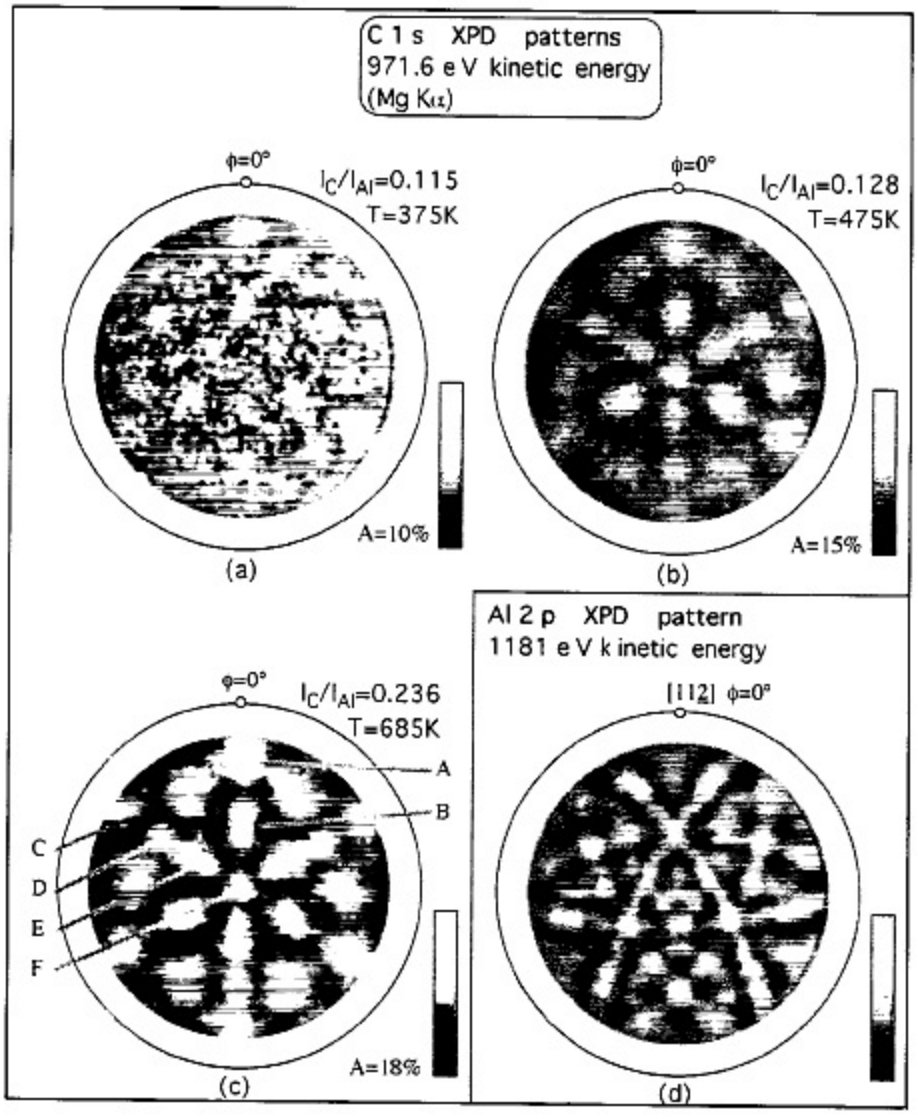

Fig. 2. XPD patterns of the C 1s signal (at 971.6 eV kinetic energy) obtained for submonolayer C films deposited at RT on Al(111) obtaining the indicated ratio between the C 1s and the Al 2p photoemission intensity and after annealing at (a) $T=375$ K, (b) $T=475$ K, (c) $T=685$ K. In (d) we show the intensity distribution pattern of Al 2p photoelectrons (at 1181 eV kinetic energy). Small open circles indicate the [11$\bar{2}$] direction of the Al(111) surface, considered as the $\theta=0^\circ$ azimuth. A smooth background is removed from the patterns and the data are three-fold averaged (see text). Anisotropy values (%) are indicated by A in each pattern.

other atoms). In fact, if the photoelectrons are coming from C atoms embedded in between the first and the second Al layer, the intensity maxima should occur at rather grazing emission. On the other hand, if the C emitter atom is located below the second layer, intensity maxima appear also close to the normal emission direction.

This observation links well with the observed polar dependence of the azimuthally averaged photoelectron intensity: if we average the C 1s intensity in a diffractogram over all azimuthal angles and plot it versus the polar angle, we obtain two different slopes below and above an annealing temperature of 475 K. In Fig. 3 we show the curves obtained for a film which was deposited at RT and subsequently annealed at 685 K. In the first

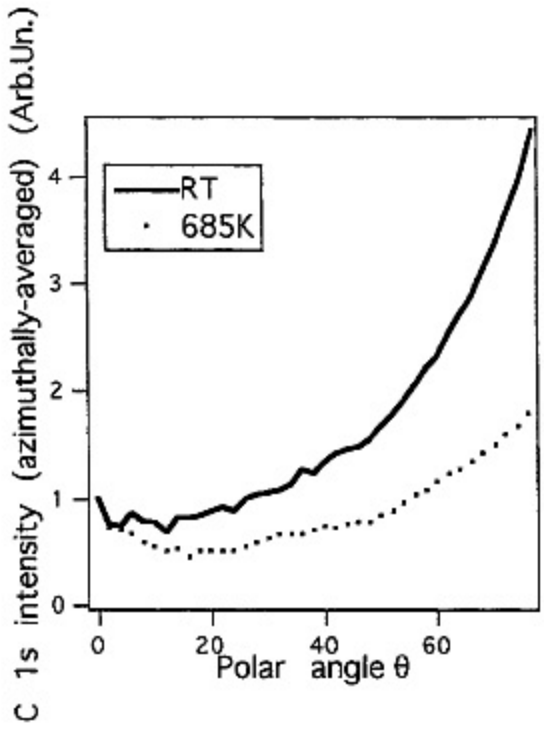

Fig. 3. Azimuthally-averaged C 1s intensity versus polar-angle for C/Al(111) as deposited (solid line) and annealed at 685 K (dotted line).

case the curve increases quite rapidly with polar angle while for the annealed sample the increasing rate is much lower (this behavior is not seen in the diffractograms in Fig. 2 because, there, the smooth dependence on the polar angle is removed to enhance contrast). In a recent work [17][2] it is shown how to link the intensity profile with the C atom depth-distribution in the surface layer: a steeper curve is an indication that the C atoms are in average closer to the surface while a flatter curve indicates that the C atoms are diffused into the bulk. By using the simplified model shown in Ref. [17] it is possible to relate the emitted intensity of C species with the near surface depth range for C emission. Thus we are able to find (by means of a fitting procedure of the curves in Fig. 3) maximum depth values of 0.5 Å and 1.7 Å for RT and the annealed film, respectively. The C atoms in an annealed sample are confined to few layers near the surface; in fact their diffusion into the bulk would result in a negative curvature.

[2] An intuitive explanation of this effect is given by the fact that when the C atoms diffuse towards the bulk the C 1s signal at grazing emission is lowered by inelastic processes which take place before the surface is reached.

4. SSC calculations

In order to determine the structure of the C/Al(111) surfaces after annealing, we performed a detailed study involving single scattering cluster (SSC) calculations and a reliability factor (*R*-factor) analysis. The SSC model used for the photoelectron diffraction calculations in this study was introduced by Friedman and Fadley [13,14] and we use it in a form that contains spherical-wave scattering and the correct s→p angular momentum final state in C 1s photoemission. The partial-wave scattering phase shifts δ_l, for scattering at C and at Al atoms are calculated by means of an algorithm based on the muffin-tin approximation [18]. Attenuation of the photoelectron wave amplitude is provided by an exponential factor of the form $\exp[-\ell/2\lambda\cos(\theta)]$, where λ is the inelastic mean free path of the photoelectrons, θ the emission angle and ℓ the distance the photoelectron travels before leaving the surface.

To estimate the agreement between experimental and calculated patterns, we performed an *R*-factor analysis [1] based on the space of multipole coefficients a_{lm} rather than emission angles (θ, ϕ). The multipole coefficients a_{lm} for the experimental and the calculated diffraction patterns $I(\theta, \phi)$ are:

$$a_{lm} = \frac{1}{4\pi} \int \chi(\theta, \phi)\, Y^*_{lm}(\theta, \phi)\, \mathrm{d}\Omega,$$

where are Y^*_{lm} the complex conjugates of the spherical harmonics, and $\chi(\theta, \phi)$ is the oscillatory part of the diffraction pattern obtained by normalization with respect to the average intensity $I_0(\theta)$ for each polar angle θ:

$$\chi(\theta, \phi) = [I(\theta, \phi) - I_0(\theta)]/I_0(\theta).$$

The *R*-factor is then obtained by summing the distance between the points in the complex plane representing the experimental and theoretical multipole coefficients a_{lm} over all l and m's

considered:

$$R = \sum_{l=0}^{l_{max}} \sum_{m=-l}^{l} |a_{lm}^{th} - a_{lm}^{exp}|.$$

We have carried out our calculations using a value of $l_{max} = 60$, that is sufficient to reproduce all fine structures present in the data.

The C 1s diffraction patterns generated from several clusters containing C and Al atoms are examined starting from the theoretical prediction by Furthmüller et al. [9] of the energetically favoured sites for C atoms. In Fig. 4 we show the simulated patterns for single atoms occupying these sites, i.e. an "*hcp in*" site, four-fold coordinated with the C atom 0.1 Å below the relaxed Al surface plane and with a 0.28 Å outward relaxation of the surrounding Al atoms (Fig. 4a); an "*fcc in*" site where the C atom is placed 0.05 Å above the surface layer with a 0.24 Å upward and 0.28 Å outward relaxation of the nearest neighbor Al atoms and a 0.14 Å upward and 0.17 Å outward relaxation of the next nearest neighbor Al atoms (Fig. 4b); an "*fcc on*" site with the atom placed 0.96 Å above the surface plane and the nearest neighbor Al atoms moved 0.17 Å upwards and 0.13 Å outwards (Fig. 4c); an "*fcc sub*" site, six-fold coordinated with the C atom half-way between the first and second layer (Fig. 4d) and with a negligible relaxation of the neighboring Al atoms. Fig. 4e gives a sketch of the situation.

It is immediately clear that none of the patterns (Figs. 4a–d) reproduces the experiment (Fig. 2). In particular, the calculated pattern for the "*fcc sub*" adsorption site (Fig. 4d) shows a forward focusing maximum marked *A'* for $\theta = 54°$ in the $\phi = 0°$ azimuth and a broad maximum marked *C'* for $\theta = 72°$ in the $\theta = 60°$ azimuth which are clearly not present in the experimental results.

The C atom positions used for the calculations presented in Fig. 4 are all rather close to the surface topmost layer. As we already noted in the previous section, the presence of intensity maxima close to the normal is evidence for diffusion of the C atoms towards the bulk or, for a C–Al bulk compound formation. This idea is supported by theory [9], predicting only a small Al lattice distortion to accommodate a C atom and by the relatively low potential barrier calculated for diffusion. Therefore, a hypothesis would be to put an isolated C atom in an Al cluster, placing it in either four-fold coordinated sites or in six-fold ones over, say, the *first four* Al layers. Having isolated C atoms no C–C scattering takes place. However, the SSC patterns (not shown) created by such a procedure have only a marginal relation with the experiment.

A second hypothesis may suggest the formation of clusters of the known Al_4C_3 carbide. It has a rhombohedral structure with hexagonal layers of Al atoms interspersed with layers of C atoms in regular stacking sequences [19] with $a = b = c = 8.55$ Å and $\alpha = 22°28'$. We performed SSC calculations using a Al_4C_3 cluster containing 160 atoms, with three Al layers and three C layers.

Fig. 5 shows the SSC pattern for the C 1s emission from the Al_4C_3 cluster with its [111]-direction aligned to the surface normal. Also in this case agreement with the experiment is poor.

Following the idea of forming C-rich clusters, we compared the XPD patterns of the annealed film with those of C films deposited on Si(001) by chemical vapor deposition [20]. In Fig. 6 the C 1s pattern from a C/Si(001) film is projected along the [111]-direction. The similarity with the pattern of Fig. 2c is quite surprising. Only minor discrepancies are discernible: the three maxima labeled "B" in Fig. 2c are more elongated for C/Al(111) than for C/Si(100). In Ref. [19] it is shown that the existence of diamond nuclei embedded in a β-SiC *milieu* is at the origin of the pattern of Fig. 6 giving us a hint towards a C-rich structure with diamond or zincblende structure. In both of these two kinds of structures C atoms are four-fold coordinated and this is in agreement with the high stability found by Furthmüller et al. [9] for tetrahedral four-fold coordinated sites for C on Al(111).

At this point, three kinds of clusters were chosen for the simulation of the C 1s emission: two zincblende C–Al clusters with C and Al surface termination, respectively, and a diamond lattice (zincblende structure with only C scatterers). To simulate the first situation we located C emitters in a cluster with zincblende structure whose (111)-surface is parallel to the one of Al(111). In two separate calculations, we used clusters formed by eight layers of atoms according to these sequences: C–Al–C–Al–C–Al–C–Al and Al–C–Al–C–

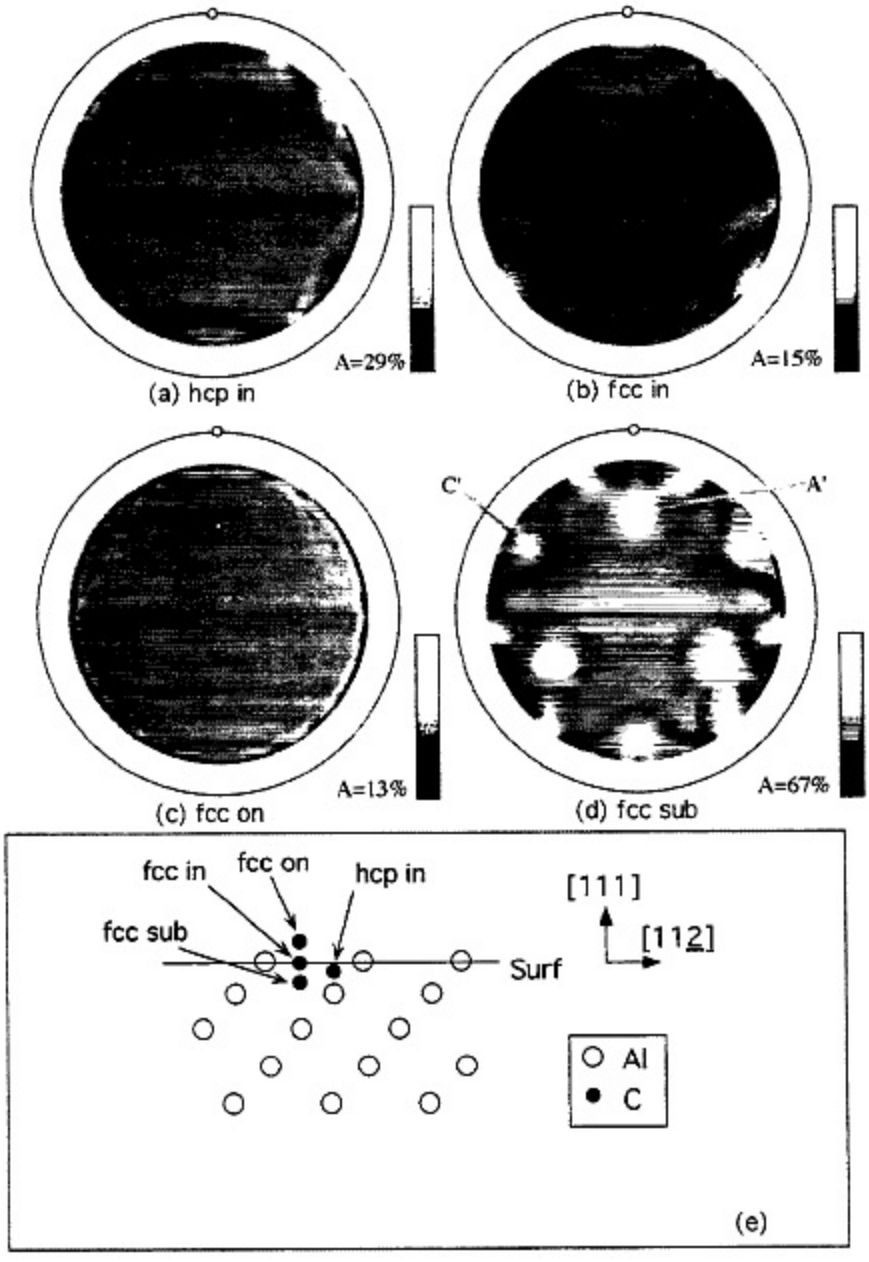

Fig. 4. Simulated diffraction patterns obtained from SSC calculations for energetically favored configurations of a C atom adsorbed on Al(111) (after Ref. [9]): (a) "*hcp in*" site, with a four-fold coordinated C atom in the Al surface plane; (b) "*fcc in* site" with the C atom 0.1 Å above the surface layer; (c) "*fcc on*" site with the C atom at 0.96 Å above the surface plane; (d) "fcc sub" site with a six-fold coordinated C atom half-way between first and second layer. The small circle indicates the [11$\bar{2}$] direction, considered as the $\phi = 0^{\circ}$ azimuth. (e) sketch of different sites. Anisotropy values (%) are indicated by A in each pattern.

Al–C–Al–C, starting with a surface plane containing C atoms in one case and with a surface plane containing Al atoms in the other one, respectively; in both cases we considered four C emitters, one in each C layer. Successively we performed the R-factor analysis, as described before, varying

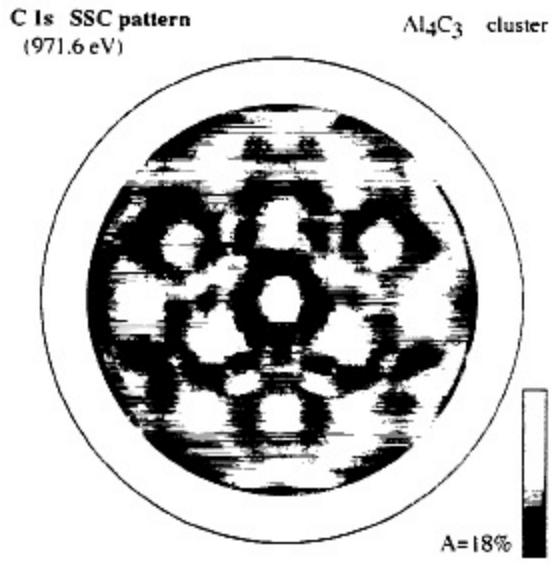

Fig. 5. SSC pattern calculated for C 1s emission from an Al_4C_3 cluster. The surface normal is aligned with the [111]-direction in the cluster. A smooth background is removed from the patterns and the data are three-fold averaged. The anisotropy value is indicated by A.

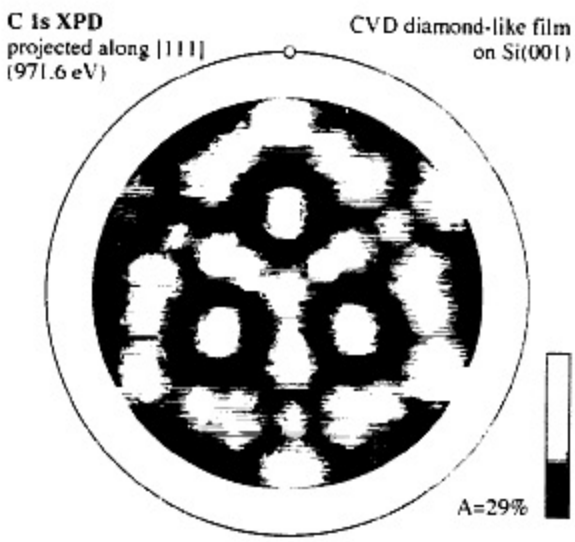

Fig. 6. XPD pattern of the C 1s signal obtained for a diamond-like C film deposited by plasma enhanced chemical vapor deposition on Si(001) (for details see Ref. [20]). The original pattern was projected along the [111]-direction in order to be directly comparable with the pattern in Fig. 2. A smooth background is removed from the pattern and the data are three-fold averaged. The small circle indicates the $[11\bar{2}]$ direction, considered as the $\phi = 0°$ azimuth. The anisotropy value is indicated by A.

four parameters: the atomic mean square displacement $\langle u_j^2 \rangle$, the intemal potential V_i, the electron mean free path λ and the lattice constant a_0. The R-factor is very sensitive to the mean free path and lattice constant variation and gives the best fit for a C-terminated cluster corresponding to an R-factor of 0.33. The optimized parameters are indicated in Table 1. The resulting C–Al distance is 1.79 Å which is 6% less than the minimal C–Al distance in natural Al_4C_3.

SSC calculations for the emission from a diamond structure were also compared with the experimental results of Fig. 2c through R-factor analysis. We used a cluster with 168 atoms placed on seven layers, each of them containing one C emitter. The lattice constant was allowed to expand in order to account for the possible Al content (the C–Al distance in Al_4C_3 varies between 1.9 and 2.3 Å while the C–C distance in diamond is 1.57 Å).

In Fig. 7a we report the calculated pattern for the best fit parameters for the expanded diamond cluster. All the features of the experimental pattern of Fig. 2c are reproduced in this pattern, with the difference that the calculation contains more fine structure. In Fig. 7b we show R-factor values versus the lattice constant.The best fit obtained using this diamond-like cluster gives a site-to-site distance of 1.93 Å corresponding to an R-factor of 0.29. The optimized parameters found in this case are indicated in Table 1.

For the interpretation of the obtained patterns we have to point out that the scattering properties of C and Al atoms are very similar in a diamond lattice. In fact, a similar SSC calculation performed for an Al cluster with diamond structure gives an only 2% worse R-factor. The best fit parameters are compatible with the following picture: the C atoms are embedded in a zincblende structure which might have no long-range site occupation order (an Al–C zincblende cluster with all Al and C atoms sitting on respective sites has a worse R-factor). From our data, it is not possible to extract the specific site occupation by C or Al atoms. The nearest neighbor distance in the best-fit cluster is equal to the distance between C and Al atoms in the natural carbide and it is smaller than the

Table 1
Optimized parameters and respective R-factor values obtained by R-factor analysis for the C-terminated zincblende C–Al cluster and for the diamond structure, marked with *AlC* and *C* superscripts, respectively. We indicate with $\langle u_j^2 \rangle$ the atomic mean square displacement, V_i the internal potential, λ the electron mean free path and a_0 the lattice constant

Values relative to zincblende cluster					Values relative to diamond cluster				
a_0^{AlC}	λ^{AlC}	V_i^{AlC}	$\langle u_j^2 \rangle$	R-factor	a_0^C	λ^C	V_i^C	$\langle u_j^2 \rangle$	R-factor
4.14 Å	4.40 Å	4.5 eV	0.030 Å^2	0.33	4.47 Å	6.00 Å	11.0 eV	0.016 Å^2	0.29

average value of the lattice constants of diamond and Al (2.21 Å).

5. Conclusions

The crystalline behavior of submonolayer C quantities on an Al(111) surface are derived from XPD measurements.

At RT, the C atoms are bound to the surface in two different chemical environments, none of them showing long or short range order. The two kinds of C atoms are present in similar quantities as revealed from the C 1s line shape.

Upon annealing above 475 K, the higher binding energy C1s component nearly disappears. While no long-range order is recovered (LEED patterns show diffuse background intensity in addition to the Al substrate spots) local order is established as it is revealed from the XPD C 1s patterns. Moreover, the features present in the XPD patterns closely resemble those of a three-dimensional structure in contrast to previous theoretical results whose predictions point to subsurface adsorption in hcp or fcc sites.

The interpretation of the XPD patterns is not straightforward. C 1s SSC calculations for the subsurface adsorption of isolated C atoms as well as for the natural Al_4C_3 rombohedral structure do not reproduce the experimental results. Starting from previous theoretical results [9] we built a three-dimensional zincblende cluster which accommodates C and Al atoms by diffusion of the former ones into the Al lattice. Calculations performed using this C–Al zincblende structure (in which C occupies tetrahedral sites) show a certain similarity with the measured patterns. The best agreement between calculations and experiment is obtained for a slightly relaxed C terminated zincblende structure in which the (111)-planes are parallel to the surface. The C–Al distance in the "expanded" cluster is 1.79 Å, 6% smaller than in the natural Al_4C_3 rhombohedral structure. A better *R*-factor is obtained using an expanded diamond cluster, i.e. with an expanded lattice parameter. The best-fit nearest neighbor distance is similar to the one of the natural carbide.

The C–Al cluster is in registry with the substrate and covers only a small part of the whole Al(111) surface since the investigated coverages is below 0.2 ML.

Our results point to a thermally activated C–Al nucleation process making the diffusion process quite different from a simple C atom diffusion. The C atom lateral diffusion on Al above 475 K has to be high enough to ensure the C–Al aggregation before inward bulk diffusion takes place. Finally, the analysis of our data from annealed C films excludes the presence of "surface" carbon and gives some hints towards two distinct hypotheses: either diamond nuclei are formed (based on the similarity between C 1s patterns from the diamond nuclei on Si(001) and our data) or we have a zincblende-type with a disordered Al and C site occupancy. Further investigations are needed to distinguish between them.

Acknowledgements

We thank G. Chiarello for the continued and helpful discussion. Skilful technical support was provided from H. Tschopp, E. Mooser, O. Raetzo, F. Bourqui and Ch. Neururer. This project has been supported by the Fonds National Suisse pour la Recherche Scientifique.

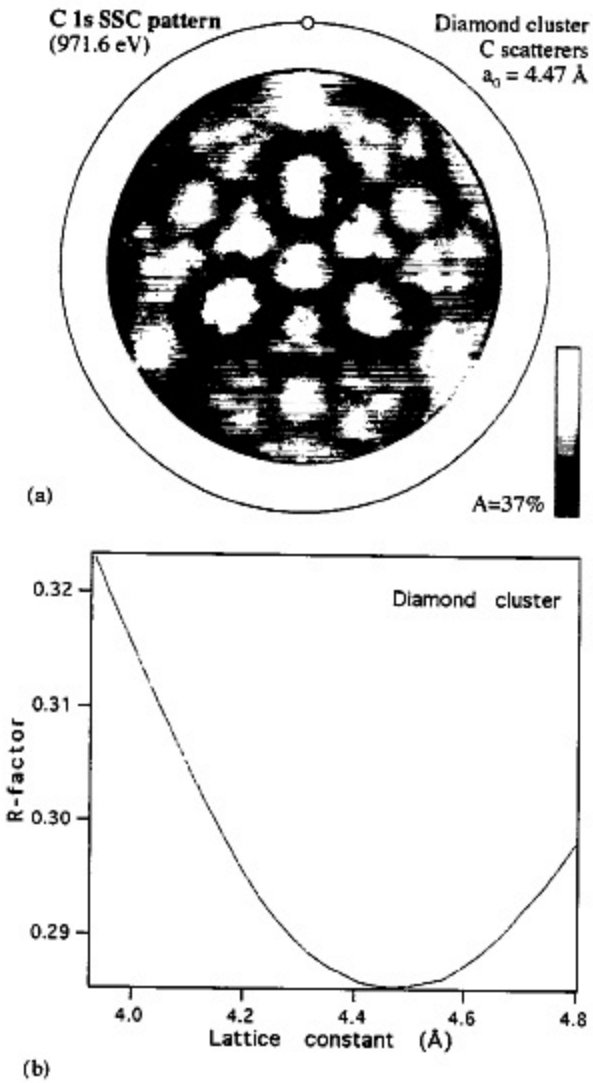

Fig. 7. (a) SSC pattern calculated for C 1s emission from a diamond cluster with a lattice parameter of 4.47 Å. A smooth background is removed from the patterns and the data are 3-fold averaged. The small circle indicates the $[11\bar{2}]$ direction, considered as the $\phi=0^{\circ}$ azimuth; (b) R-factor values versus lattice constant a_0^C (for fixed optimized values of λ_C, V_i^C, $\langle u_j^2 \rangle$) of the diamond structure that gives rise to the SSC pattern in (a). The anisotropy value is indicated by A.

References

[1] R. Fasel, P. Aebi, J. Osterwalder, L. Schlapbach, R.G. Agostino, G. Chiarello, Phys. Rev. B 50 (1994) 14516.
[2] Y. Huttel, P. Soukiassian, P.S. Mangat, Z. Hurych, Surf. Rev. Lett. 2 (1995) 549.
[3] H. Brune, J. Wintterlin, R.J. Behm, G. Ertl, Phys. Rev. Lett. 68 (1992) 624.
[4] C.F. McConville, D.L. Seymour, D.P. Woodruff, S. Bao, Surf. Sci. 188 (1987) 1.
[5] J. Jacobsen, B. Hammer, K.W. Jacobsen, J.K. Nørskov, Phys. Rev. B 52 (1995) 14954.
[6] J.E. Müller, Surf. Sci. 178 (1986) 589.
[7] I.P. Batra, L. Kleinman, J. Electron Spectrosc. Relat. Phenom. 33 (1984) 175.
[8] H. Brune, J. Wintterlin, G. Ertl, R.J. Behm, Europhys. Lett. 13 (1990) 123.
[9] J. Furthmüller, G. Kresse, J. Hafner, R. Stumpf, M. Scheffler, Phys. Rev. Lett. 74 (1995) 5084.
[10] J. Osterwalder, P. Aebi, R. Fasel, D. Naumović, P. Schwaller, T. Kreutz, L. Schlapbach, T. Abukawa, S. Kono, Surf. Sci. 331 (1995) 1002.
[11] C.S. Fadley, in: S.G. Davison (Ed.), Progress in Surface Science, vol. 16, Pergamon, New York, 1984, p. 275.
[12] C.S. Fadley, in: R.Z. Bachrach (Ed.), Synchrotron Radiation Research: Advances in Surface Science, chap. 11, Plenum, New York, 1990.
[13] D.J. Friedman, C.S. Fadley, J. Electron Spectr. Relat. Phenom. 51 (1990) 689.
[14] J.J. Rehr, R.C. Albers, Phys. Rev. B 41 (1990) 8139.
[15] J. Osterwalder, T. Greber, A. Stuck, L. Schlapbach, Phys. Rev. B 44 (1991) 13764.
[16] D. Naumović, A. Stuck, T. Greber, J. Osterwalder, L. Schlapbach, Phys. Rev. B 47 (1993) 7462.
[17] R.G. Agostino, O.M. Küttel, P. Aebi, R. Fasel, J. Osterwalder, L. Schlapbach, J. Appl. Phys. 80 (1996) 2181.
[18] J.B. Pendry, Low Energy Electron Diffraction, Academic, London, 1974.
[19] G.A. Jeffrey, V.Y. Wu, Acta Cryst. 16 (1963) 559.
[20] E. Schaller, O.M. Küttel, P. Aebi, L. Schlapbach, Appl. Phys. Lett. 67 (1995) 1533.